

1
2
3
4
5
6
7
8
9
10
11
12
13
14
15
16
17
18
19
20
21
22
23
24
25
26
27
28
29
30
31
32

IPSE, a parasite-derived host immunomodulatory protein, is a potential therapeutic for hemorrhagic cystitis

Running head: IPSE as potential hemorrhagic cystitis therapy

Rebecca S. Zee ^{*}, †, Evaristus C. Mbanefo^{*}, †, Loc H. Le†, Luke F. Pennington‡, Justin Odegaard§, Theodore S. Jardetzky‡, Abdulaziz Alouffi¶, Jude Akinwale||, Franco H. Falconell, Michael H. Hsieh^{*}, †, #

^{*} Division of Urology, Children's National Medical Center, Washington DC, USA

† Bladder Immunology Group, Biomedical Research Institute, Rockville, MD, USA

‡ Department of Structural Biology, Stanford University School of Medicine, Stanford, CA, USA

§ Guardant Health, Redwood City, CA, USA

¶ Life science and Environment Sector, King Abdulaziz City for Science and Technology (KACST), Riyadh, Saudi Arabia

|| Division of Molecular Therapeutics and Formulation, School of Pharmacy, University of Nottingham, Nottingham, United Kingdom

The George Washington University, Washington, DC, USA

Correspondence:

Michael H. Hsieh
Children's National Medical Center
111 Michigan Ave NW
Washington, D.C. 20010
Telephone: 202-476-1293
Fax: 202-476-4739
Email: mhsieh@childrensnational.org

Figure count: 6

33 **Abbreviations**

34	CFSE	5-(and 6)-Carboxyfluorescein diacetate succinimidyl ester
35	IPSE	Interleukin-4 inducing principle from <i>Schistosoma mansoni</i> eggs
36	MESNA	2-mercaptoethanesulfonic acid
37	NLS	Nuclear localization sequence

38 **Abstract**

39 Chemotherapy-induced hemorrhagic cystitis is characterized by bladder pain and
40 voiding dysfunction caused by hemorrhage and inflammation. Novel therapeutic options
41 to treat hemorrhagic cystitis are needed. We previously reported that systemic
42 administration of the *Schistosomiasis haematobium*-derived protein H-IPSE^{H06} (IL-4-
43 inducing principle from *Schistosoma mansoni* eggs), is superior to 3 doses of MESNA in
44 alleviating hemorrhagic cystitis. Based on prior reports by others on *S. mansoni* IPSE
45 (M-IPSE) and additional work by our group, we reasoned that H-IPSE mediates its
46 effects on hemorrhagic cystitis by binding IgE on basophils and inducing IL-4
47 expression, promoting urothelial proliferation, and translocating to the nucleus to
48 modulate expression of genes implicated in relieving bladder dysfunction. We
49 speculated that local bladder injection of the *S. haematobium* IPSE ortholog IPSE^{H03},
50 hereafter called H-IPSE^{H03}, might be more efficacious in preventing hemorrhagic cystitis
51 compared to systemic administration of IPSE^{H06}. We report that H-IPSE^{H03}, like M-IPSE
52 and H-IPSE^{H06}, activates IgE-bearing basophils in an NFAT reporter assay, indicating
53 activation of the cytokine pathway. Further, H-IPSE^{H03} attenuates ifosfamide-induced
54 increases in bladder wet weight in an IL-4-dependent fashion. H-IPSE^{H03} relieves
55 hemorrhagic cystitis-associated allodynia and modulates voiding patterns in mice.
56 Finally, H-IPSE^{H03} drives increased urothelial cell proliferation suggesting that IPSE
57 induces bladder repair mechanisms. Taken together, H-IPSE^{H03} may be a potential
58 novel therapeutic to treat hemorrhagic cystitis by basophil activation, attenuation of
59 allodynia and promotion of urothelial cell proliferation.

60 **Key words:** IL-4, IPSE, hemorrhagic cystitis, schistosomiasis

61 Introduction

62 Ifosfamide and other alkylating chemotherapy agents are used in a wide variety
63 of malignancies including leukemias, soft tissue sarcomas, and testis cancer. The liver
64 metabolizes ifosfamide into acrolein, which is excreted in the urine and has a
65 deleterious effect on the urothelium. Hemorrhagic cystitis is characterized by bladder
66 edema, hemorrhage, urothelial denudation, and infiltration of inflammatory cells. This
67 condition affects up to 40% of ifosfamide-exposed patients, resulting in hematuria,
68 dysuria, bladder spasms, and urinary frequency (10). Hemorrhagic cystitis is a
69 challenging condition to manage, and often requires hospitalization and invasive
70 treatments (18).

71 Accordingly, strategies to attenuate ifosfamide-induced hemorrhagic cystitis,
72 such as administration of 2-mercaptoethanesulfonic acid (MESNA), bladder irrigation, or
73 hyperhydration often achieve suboptimal protection for patients (18). Despite use of
74 existing therapies, a majority of patients have symptomatic and/or histologic evidence of
75 hemorrhagic cystitis (16). As an alternative to current management approaches,
76 Macedo *et al.* reported that administration of recombinant interleukin-4 (IL-4) attenuated
77 the effects of ifosfamide in a mouse model of hemorrhagic cystitis (17). The importance
78 of IL-4 in this model was demonstrated by administration of anti-IL4 antibody to
79 ifosfamide-exposed, wild type mice and administration of ifosfamide to IL-4-deficient
80 mice, both of which resulted in worsened hemorrhagic cystitis (23). Interestingly,
81 ifosfamide administration increased endogenous production of IL-4, suggesting the
82 existence of intrinsic regulatory mechanisms to control inflammation in response to
83 ifosfamide (17). However, systemic administration of IL-4 to treat hemorrhagic cystitis

84 may not be a realistic option due to pleiotropic effects and a short *in vivo* half-life of this
85 cytokine (20). Therefore, alternative strategies to increase expression of IL-4 would be
86 needed in order to leverage this cytokine for therapeutic treatment of hemorrhagic
87 cystitis.

88 One alternative may be the interleukin-4 inducing principle from *Schistosoma*
89 *mansoni* eggs (IPSE), the most abundant protein secreted by *S. mansoni* eggs. IPSE
90 attenuates inflammation via multiple mechanisms, including binding immunoglobulins to
91 stimulate IL-4 release, sequestering chemokines, and translocating to the nucleus to
92 modulate transcription (13, 19, 22, 27). We have previously reported that similar to the
93 *S. mansoni* ortholog of IPSE, M-IPSE, several *S. haematobium* orthologs, referred
94 hereafter as H-IPSE, bind to IgE on mast cells and basophils and upregulate the
95 expression of IL-4 (22). Through sequencing of *S. haematobium* cDNA transcripts, we
96 identified two main clades of H-IPSE – H-IPSE^{H03} and H-IPSE^{H06} --with conservation of
97 functional domains present in M-IPSE, such as 7 cysteines important for intra- and
98 intermolecular bonds, a nuclear translocation sequence (NLS), and 2 N-linked
99 glycosylation motifs. IPSE has a homodimeric structure with a molecular weight of 38-
100 40 kDa. Importantly, both H-IPSE^{H03} and H-IPSE^{H06} translocate into urothelial cell nuclei
101 (22).

102 Initial animal experiments with H-IPSE focused on the effect of systemic
103 administration of H-IPSE^{H06} by tail vein injection (19). Tail vein injection of H-IPSE^{H06}
104 attenuates ifosfamide-induced bladder hemorrhage in an IL-4 and NLS-dependent
105 manner. Furthermore, mice treated with H-IPSE^{H06} prior to ifosfamide exposure
106 demonstrated fewer spontaneous pain behaviors and had a higher threshold for evoked

107 pain responses (19). We speculated that direct injection of IPSE into the bladder wall
108 would have multiple advantages over intravenous injection, including avoidance of side
109 effects caused by systemic administration (although none have been identified to date),
110 and potentially decreased dosage to achieve a therapeutic effect. Further, experiments
111 in our lab have shown that H-IPSE^{H03} induces a more robust proliferative response *in*
112 *vitro* when compared to H-IPSE^{H06} (unpublished data) making H-IPSE^{H03} a more
113 attractive target to investigate the role of H-IPSE^{H03} in promoting urothelial repair. The
114 aim of this work was to determine whether direct bladder wall injection of H-IPSE^{H03}
115 attenuates bladder inflammation, voiding dysfunction and pain in a mouse model of
116 hemorrhagic cystitis.

117

118 **Materials and Methods**

119 Mice

120 Six to 8-week-old female C57BL/6 mice (Charles River Laboratories, Wilmington,
121 MA) were housed in cages with free access to water and standard chow and 12 hour
122 light-dark cycles. Mice were acclimated for at least 7 days prior to experimentation. The
123 animal protocol (#18-03) was approved by the Institutional Animal Care and Use
124 Committee at the Biomedical Research Institute (Rockville, MD). Our institutional animal
125 care and use committee guidelines follow the U.S. Public Health Service Policy on
126 Human Care and Use of Laboratory Animals.

127

128 Bladder wall injections

129 Mice received a single bladder wall injection of H-IPSE^{H03} 24 hours prior to
130 exposure to ifosfamide. Mice were anesthetized with 2% continuous isoflurane on a
131 heating pad. Procedures were performed using sterile technique. For pain control, 0.1
132 mg/kg buprenorphine and 0.1 mg/kg bupivacaine were injected subcutaneously. A
133 midline laparotomy was performed sharply and the bladder delivered through the
134 incision. Mice were divided into 3 groups receiving sham, control or IPSE. A 30-gauge
135 needle was used to inject a 1:1 v/v mixture of Low Growth Factor Matrigel (Corning,
136 Corning, New York) and PBS containing 25 µg mouse albumin (control) or 25 µg H-
137 IPSE (IPSE) (Figure 1). Sham mice received a midline laparotomy only. Incisions were
138 closed in 2 layers using 5-0 Vicryl on the abdominal wall and 5-0 silk to close skin.
139 Bacitracin was applied to the incision. The mice were recovered on a heating pad.
140 Twenty-four hours later mice were injected with 400 mg/kg ifosfamide (Sigma-Aldrich,

141 St. Louis, MO). Mice who received anti-IL4 antibody (inVivoMab 11B11, BioXcell, West
142 Lebanon, NH) received 10 ng by intraperitoneal (IP) injection 30 minutes before
143 ifosfamide. Control mice received IP injections of phosphate-buffered saline (PBS). At
144 12 hours, mice were euthanized, their bladders removed and weighed. Bladders were
145 then subjected to additional analysis detailed below. Each experiment was performed
146 on 3-4 mice per group. Figures are pooled from 3 experiments.

147 Tail vein injections

148 Mice were anesthetized with 2% continuous isoflurane on a heating pad. A 30-
149 gauge needle was used to inject PBS containing 25 µg mouse albumin or 25 µg H-
150 IPSE^{H03} (IPSE) in PBS. The mice were recovered on a heating pad. Twenty-four hours
151 later mice were injected with 400 mg/kg ifosfamide (Sigma-aldrich, St. Louis, MO). Mice
152 who received anti-IL4 antibody (inVivoMab 11B11, BioXcell, West Lebanon, NH)
153 received 10 ng by intraperitoneal (IP) injection 30 minutes before ifosfamide. Control
154 mice received IP injections of phosphate-buffered saline (PBS). At 12 hours, mice were
155 euthanized, bladders were removed and weighed.

156 Recombinant IPSE protein

157 Recombinant IPSE protein was generated as previously described (1,2). One
158 milligram of plasmid DNA was purified using a GeneElute HP endotoxin-free plasmid
159 Maxiprep kit (Sigma-Aldrich), and incubated with 3 mg linear 25 kDa polyethylenimine
160 (PolySciences, Warrington, PA) at 1 mg/mL. Finally, the plasmid was diluted in 10 mL
161 sterile PBS for each transfection in 1L. Human embryonic kidney 293-6E cells (7)
162 expressed secreted recombinant protein for 5 days in suspension culture using

163 FreeStyle 293 Medium (Thermo Fisher Scientific, Waltham, MA, USA) (Figure 2A).
164 Protein was purified over 10 mL Ni-NTA resin (Qiagen, Germantown, MD, USA),
165 washed with 25 mM imidazole PBS, pH 7.4, and eluted with 300 mM imidazole PBS, pH
166 7.4 containing 50 mM arginine. Eluted protein was concentrated with an Amicon Ultra
167 Centrifugal Filter Unit (EMD Millipore, Billerica, MA, USA) followed by purification with a
168 Hiload 16/600 Superdex 200 Column (GE Healthcare, Waukesha, WI, USA). Nuclear
169 localization mutants were generated using site-directed mutagenesis. These mutants
170 (124-PKRRRTY-130 to 124-PKAAATY-130) disrupted the C-terminal NLS (NLS; H-
171 IPSE^{H03NLS}) (2). To decrease the risk of pyrogen contamination, FPLC machines and
172 Hiload columns were cleaned with 0.5 M NaOH for a minimum of 2 hours continuous
173 flow and then washed with PBS, pH 7.4.

174 SDS-PAGE and Western blotting

175 Purified protein was separated on 4-20% gradient gels by SDS-PAGE in 15 μ L
176 aliquots (Mini-Protean TGX Precast Gels, Biorad). Separated proteins were then
177 transferred to a 0.2 μ M nitrocellulose membrane. Membranes were incubated in
178 blocking buffer for 1 hour (5% [wt/vol] dried skim milk, 0.01% [vol/vol] Tween 20, and
179 Tris-buffered saline [TBS]) on a shaker at room temperature. Primary antibody was
180 mouse anti-His (GE-Healthcare) diluted at 1:500 and incubated overnight at 4°C
181 followed by washing in TBS containing 1% Tween 20 for 5 min x 3. Membranes were
182 then incubated with secondary antibody--HRP-conjugated anti-mouse IgG (Sigma-
183 Aldrich) -- for 1 hour at room temperature followed by 3 additional washes. Imaging was
184 performed using Pierce ECL Western Blotting Reagent (ThermoScientific Fisher) on a
185 Fuji LAS4000 imager.

186 Basophil activation with recombinant M-IPSE, H-IPSE^{H03} and H-IPSE^{H06}

187 Basophil activation was quantified as previously described (28), using a
188 luciferase based humanized IgE reporter system. The cell line reports IgE-dependent
189 NFAT translocation to the nucleus, which is indicative of induction of cytokine
190 transcription (8). RS-ATL8 cells were counted and 10^5 cells were cultured in 10 mL
191 MEM (GIBCO, USA), supplemented with 5% vv v/v heat-inactivated FCS (GIBCO,
192 USA), 100 U/mL penicillin, and 100 µg/mL streptomycin (Sigma, UK) and 2 mM L-
193 glutamine (Sigma, UK) for 48 hours. Cells were grown in 75 cm² flasks at 37°C in a
194 humidified atmosphere with 5% carbon dioxide. 1 mg/mL G418 (Fisher
195 ThermoScientific, UK) and 600 µg/mL hygromycin B (Invitrogen, Paisley, UK) were used
196 to maintain expression of human FcεRI genes and NFAT-luciferase, respectively. Prior
197 to testing, cells were incubated overnight with a 1:50 dilution of human serum from a
198 healthy atopic donor as a source of IgE. The next day, the sensitized basophils were
199 stimulated with recombinant M-IPSE, H-IPSE^{H03} or H-IPSE^{H06} at concentrations ranging
200 from 5 to 5000 ng/mL. Luciferase assays were performed 4 hours after activation with
201 ONE-Glo Luciferase Assay System (Promega, UK), following the manufacturer's
202 instructions. The luciferase substrate was added and chemiluminescence was
203 measured using a microplate reader (Tecan, Spark™ 10M multimode microplate
204 reader, Tecan, Männedorf, Switzerland) within 30 minutes.

205 Pain assessment

206 Visceral pain scores were assigned as previously described (10). The observer
207 was blinded to mouse treatment assignments prior to assessments. Mice were placed in
208 clean cages and acclimated for 30 min. For spontaneous pain scoring, mice were

209 observed for 60 seconds and given a cumulative spontaneous pain score based on the
210 following: (0) – normal; (1) – piloerection; (2) – labored breathing; (3) – ptosis; (4) –
211 licking of abdomen (not grooming); (5) – rounded back. The maximum possible visceral
212 pain score is 15. Pain scores were collected at baseline (prior to bladder wall injection),
213 and 10 hours after ifosfamide was administered.

214 Von Frey filament testing

215 Evoked pain scores were collected in a blinded fashion to assess for referred
216 hyperalgesia. We adopted the up-down approach as previously described (6, 15). An
217 electronic Von Frey filament (BioSeb, Pinellas Park, Florida) was applied to the right
218 hind footpad of the mouse for 5 seconds until the mouse displayed rapid withdrawal of
219 the paw, jumping, or licking of the paw. The 50% withdrawal threshold was then
220 calculated from an average of 3 measurements. Results are tabulated as the difference
221 between baseline and post-ifosfamide values.

222 Voided Spot on Paper Assay

223 Voided spot on paper assays were performed as previously described (1, 9, 12,
224 30). Mice were placed in individual cages 2 hours after ifosfamide or PBS
225 administration. Whatman paper was cut to the dimensions of the cage floor. The paper
226 was covered with wire mesh to prevent mice from tearing or ripping the paper. Food
227 was provided *ad libitum* in the form of regular chow. Water was not provided to prevent
228 fluid dripping onto the paper and causing data loss or artifact. Mice were placed under
229 quiet conditions for 4 hours. They were then returned to normal housing conditions after
230 completion of the experiment. The pieces of Whatman paper were converted to .tiff

231 images using UV transillumination (Bio-Rad, Hercules, CA). Image analysis was
232 performed with ImageJ Fiji (<https://fiji.sc/>). Corner voiding was assessed by assigning
233 5% of the total paper area to each corner. Central voiding was assessed by assigning
234 40% of the total area to the center of the filter paper.

235 *In vitro* proliferation assays

236 MB49 cells were counted and plated with equal numbers of cells in each well. H-
237 IPSE^{H03} or H-IPSE^{H03NLS} were added to the cell media at the following concentrations:
238 0.0655 pmol (1 ng/ml), 0.655 pmol (10 ng/ml), 6.55 pmol (100 ng/ml), 65.5 pmol (1000
239 ng/ml), or PBS for control. 5-(and 6)-Carboxyfluorescein diacetate succinimidyl ester
240 (CFSE) assays were then performed according to manufacturer's instructions
241 (ThermoFisher Scientific, Waltham, MA). One mL of a single cell suspension for each
242 experimental condition was then acquired on a BD FACSCanto II machine (BD
243 Biosciences, San Jose, CA). Flow cytometric analysis was performed using FlowJo
244 software (Ashland, OR).

245 Statistical analysis

246

247 One-way ANOVA or Student's t-test were utilized as appropriate. *Post hoc* testing was
248 performed with Bonferroni test. A p-value of less than 0.05 was considered statistically
249 significant.

250 **Results**

251 **Recombinant H-IPSE^{H03} and H-IPSE^{H06} proteins activate IgE-bearing basophils *in*** 252 ***vitro***

253 We previously demonstrated that M-IPSE activates basophils *in vitro* through NF-
254 AT (28). This pathway is implicated in basophil and mast cell expression of IL-4, which
255 we have observed *in vivo* in mice administered H-IPSE^{H06} (19). Moreover, we have also
256 noted that ifosfamide-challenged mice given H-IPSE^{H06} are protected from several
257 pathogenic aspects of hemorrhagic cystitis in an IL-4-dependent fashion (19). Thus, we
258 sought to demonstrate that H-IPSE^{H03} and H-IPSE^{H06}, which are both *S. haematobium*
259 orthologs of M-IPSE, also stimulate IL-4-associated reporter gene expression *in vitro*.
260 We first purified recombinant H-IPSE^{H03} and H-IPSE^{H06} from transfected HEK293-6E
261 cells. Western blots under non-reducing conditions identified a band with a molecular
262 weight of 38-40 kDa which corresponds to the homodimeric H-IPSE structure (Figure
263 2A). Recombinant H-IPSE^{H03} and H-IPSE^{H06} protein was then incubated with IgE-
264 loaded basophils. This resulted in NF-AT activation, which is associated with IL-4
265 secretion in basophils (Figure 2B). Having confirmed that H-IPSE^{H03} triggers IL-4-
266 associated pathways in cultured basophils, we next sought to determine the therapeutic
267 efficacy of H-IPSE^{H03} in the mouse model of ifosfamide-induced hemorrhagic cystitis.

268 **H-IPSE^{H03} dampens chemotherapy-induced increases in bladder wet weight**

269 We assessed for an increase in bladder wet weight caused by hemorrhage,
270 edema and cellular infiltration following ifosfamide injection. Ifosfamide administration
271 caused a statistically significant increase in bladder wet weight compared to controls
272 (Figure 3A, 3B; n=8, p<0.001) A single H-IPSE^{H03} bladder wall injection significantly

273 reversed the increase in bladder wet weight caused by ifosfamide in bladder wall
274 injected mice but not mice that received tail vein injection ($p=0.02$ and N.S.,
275 respectively). The beneficial effect of IPSE^{H03} on bladder wet weight was reversed by
276 anti-IL4 antibody ($p<0.001$). However, IPSE^{H03NLS} (H-IPSE^{H03} with a non-functional
277 nuclear localization sequence) also ameliorated ifosfamide-induced increases in bladder
278 wet weight, regardless of mode of administration, suggesting that the therapeutic effect
279 of IPSE on bladder wet weight is mediated by IL-4, but not dependent on IPSE
280 translocation into the nucleus. Histological analysis was not possible in this model due
281 to the effects of inflammation induced by bladder wall injection in this surgical model.

282 Tail vein injection results were distinct from bladder wall injection in two ways.
283 After tail vein H-IPSE^{H03} injection bladder wet weights decreased but remained
284 significantly higher than non-ifosfamide-exposed controls (Figure 2B; $p=0.03$).
285 Furthermore, administration of H-IPSE^{NLS} to ifosfamide-treated mice demonstrated a
286 downward trend in bladder wet weight that was not significant compared to mice given
287 only ifosfamide.

288 **H-IPSE^{H03} abrogates evoked pain responses in chemotherapy-treated mice**

289 We next sought to determine whether H-IPSE^{H03} administration had an effect on
290 ifosfamide-induced bladder pain. We first measured referred hyperalgesia using von
291 Frey filament testing. Mice injected with ifosfamide had greater evoked pain responses
292 than those of control mice (Figure 4). H-IPSE^{H03} bladder wall injection increased the
293 withdrawal threshold, i.e., reversed allodynia caused by ifosfamide injection ($p<0.05$).
294 When neutralizing anti-IL-4 antibody was co-administered with H-IPSE^{H03}, the protective
295 effect of H-IPSE^{H03} was attenuated ($p<0.05$). Likewise, injection of H-IPSE^{H03NLS}, which

296 cannot translocate to the nucleus, also featured a decreased analgesic effect compared
297 to IPSE^{H03} (p<0.05). H-IPSE^{H03} had no effect on referred hyperalgesia when
298 administered via tail vein injection (data not shown)

299 **H-IPSE^{H03} does not significantly affect abnormal ifosfamide-induced voiding**
300 **patterns in mice**

301 C57BL/6 mice demonstrate characteristic voiding behavior of voiding
302 preferentially in cage corners whereas urothelial injury significantly increases central
303 cage voiding (30). We assessed for voiding dysfunction caused by ifosfamide based on
304 the percentage of overall voids in the corners of cages. When mice received ifosfamide,
305 the percentage of corner voids was significantly decreased (Figure 5). H-IPSE^{H03}
306 increased the frequency of corner voiding in the presence of ifosfamide, but this was not
307 a statistically significant finding. Administration of α -IL4 antibody reversed the effect of
308 H-IPSE^{H03} on corner voiding and was not significantly different from ifosfamide
309 treatment (p=0.07 vs. control).

310 Ifosfamide administration non-significantly increased the percentage of voids in
311 the central area of cages (Figure 5B). H-IPSE^{H03}, α -IL4 antibody or H-IPSE^{H03NLS} did not
312 have a significant effect on central voiding. H-IPSE^{H03NLS}-treated mice were not
313 significantly different from ifosfamide-treated or control mice. Tail vein injection of H-
314 IPSE^{H03} did not significantly improve or alter voiding patterns in ifosfamide-treated mice
315 (Data not shown).

316 **H-IPSE^{H03} promotes proliferation of urothelial cells *in vitro***

317 Given the beneficial effects of H-IPSE^{H03} on ifosfamide-induced bladder wet
318 weight increases and pain, as well as prior data indicating a direct effect of H-IPSE^{H03}
319 on urothelial cells (19), we assessed the effect of H-IPSE^{H03} on urothelial cell
320 proliferation by co-incubating H-IPSE^{H03} with the MB49 (mouse carcinoma-derived
321 urothelial) cell line. H-IPSE^{H03} significantly increased cell proliferation over two
322 successive daughter cell generations compared to controls (Figure 5A; *p<0.05,
323 **p<0.01, ***p<0.0001; n=8). This held true across a range of H-IPSE^{H03} concentrations.
324 In contrast, co-incubation of cells with H-IPSE^{H03NLS} did not cause increased
325 proliferation over that of controls (Figure 5B).

326 **Discussion**

327 Hemorrhagic cystitis is a common sequela of alkylating chemotherapy, affecting
328 up to 40% of patients who receive ifosfamide or cyclophosphamide (16). Once
329 established, hemorrhagic cystitis is a challenging-to-manage entity characterized by
330 widespread bladder inflammation and leading to hematuria, dysuria, small volume
331 voids, urinary frequency, and bladder spasms. Currently available medical therapy,
332 MESNA, has a narrow therapeutic window as it can only be administered immediately
333 before and during chemotherapy. MESNA can cause hypersensitivity reactions and is
334 ineffective in treating hemorrhagic cystitis once it has been established (2, 24, 26).
335 Therefore, novel therapies need to be developed to fulfill this unmet need.

336 One source of new drugs for hemorrhagic cystitis may be derived from
337 *Schistosoma haematobium*. Urogenital schistosomiasis is a parasitic disease in which
338 *Schistosoma haematobium* worms lay eggs in the bladder and other pelvic organs.
339 Deposited eggs must traverse the host bladder wall in order to be released in the urine.
340 Although urogenital schistosomiasis itself causes a form of hemorrhagic cystitis,
341 hematuria can be variable or even absent (29). We reasoned that host
342 immunomodulation by *S. haematobium* egg products allow the parasite to complete its
343 life cycle without causing severe morbidity to its host, including hemorrhagic cystitis
344 (11). Specifically, we postulated that *S. haematobium* eggs can accomplish this by
345 secreting H-IPSE orthologs in order to modulate the host immune response.

346 In a prior study we demonstrated the clinical potential of exploiting the anti-
347 inflammatory and analgesic properties of H-IPSE^{H06} (19). A single intravenous dose of

348 H-IPSE^{H06} was superior to MESNA in alleviating bladder hemorrhage in ifosfamide-
349 treated mice (19).

350 Clinical translation of H-IPSE^{H06}, H-IPSE^{H03}, and other IPSE orthologs will require
351 large-scale recombinant protein production. Herein we show that H-IPSE^{H03} and H-
352 IPSE^{H06} can be purified from mammalian HEK293T-6E cells. Furthermore, we
353 demonstrate that, like M-IPSE, H-IPSE^{H03} and H-IPSE^{H06} trigger IgE-bearing basophil
354 NF-AT activation *in vitro*, which in turn is linked to IL-4 secretion. H-IPSE^{H03} injected into
355 the mouse bladder wall attenuates ifosfamide-induced increases in bladder wet weight
356 in an IL-4 and NLS-dependent fashion. This suggests that H-IPSE^{H03} reduces
357 ifosfamide-induced edema, cellular infiltration, and/or hemorrhage (pathologic
358 processes which can increase bladder wet weight). When H-IPSE^{H03} was administered
359 via tail vein, ifosfamide-induced increases in bladder wet weight were unaffected.
360 Unsurprisingly, there was neither an IL-4-dependent nor nuclear translocation-
361 dependent effect compared to controls. This is consistent with our prior report that
362 intravenous administration of H-IPSE^{H06} did not affect ifosfamide-mediated increases in
363 bladder wet weight (19). There are several possible explanations for these differences
364 in effects of bladder wall versus intravenous injections. For instance, bladder wall
365 injections themselves may cause an increase in hemorrhage, and bladder mass due to
366 the added weight of the matrigel. This may make it more difficult to discern weight
367 differences between groups when compared to tail vein injection. Furthermore, bladder
368 wall injection of H-IPSE^{H03} may result in high local concentrations but low systemic
369 levels. We have previously reported that peripheral basophils may play a role in IPSE's
370 therapeutic effects in hemorrhagic cystitis (19). Recruitment of circulating basophils to

371 the site of inflammation and subsequent IL-4 release may be dependent on the action of
372 H-IPSE outside of the bladder. Conversely, it is possible that the higher local H-IPSE^{H03}
373 concentrations achieved by bladder wall injection may more effectively activate bladder
374 mast cells, basophils, and other cell types critical for therapeutic effects.

375 Another explanation for the different phenotypes observed between H-IPSE^{H03}
376 and H-IPSE^{H06} is that variations in the sequence, and therefore, function of IPSE
377 proteins have evolved such that different orthologs of H-IPSE are secreted to perform
378 different host-modulatory functions. Both orthologs of H-IPSE are homologous to M-
379 IPSE in that they both conserve the C-terminal nuclear localization sequence as well as
380 7 cysteines which are responsible for forming disulfide bonds to create a homodimeric
381 structure (22). Characterization of sequence/structure-function relationships of individual
382 orthologs of H-IPSE is the subject of continued investigation.

383 Referred hyperalgesia is a unique feature of visceral pain which causes normally
384 non-painful stimuli to feel painful, even in anatomically distant locations.
385 Cyclophosphamide/ifosfamide administration in rodents is a well-established model of
386 referred hyperalgesia (3–5). We have previously reported that intravenous delivery of
387 H-IPSE^{H06} alleviates visceral and referred pain in ifosfamide-treated mice (19). In a
388 similar fashion, bladder wall-injected H-IPSE^{H03} alleviated referred hyperalgesia in an
389 IL-4 and NLS-dependent fashion. Post-operative pain did not affect the differences
390 observed with H-IPSE^{H03} administered via bladder wall injection, as we were able to
391 demonstrate a statistically significant increase in pain threshold (i.e., decreased referred
392 hyperalgesia) in ifosfamide-treated mice who received H-IPSE^{H03}. This suggests that
393 bladder wall-injected H-IPSE^{H03} may have alleviated ifosfamide- and/or surgery-induced

394 pain. Tail vein injection of H-IPSE^{H03} did not result in a significant difference between
395 treatment groups (data not shown).

396 The voided spot on paper assay is a well-established, reliable model to assess
397 lower urinary tract function in mice (1, 9, 12, 30). The characteristic voiding patterns of
398 C57BL/6 mice consist of large volume voids in the corners of cages, whereas bladder
399 injury causes mice to void at non-corner edges or the center of cages (30). We
400 demonstrated that ifosfamide exposure alters voiding behavior by significantly
401 decreasing corner voiding. This was non-significantly reversed by H-IPSE^{H03} bladder
402 wall injection. Ifosfamide-treated mice tended to void in the central part of the cage,
403 although this was not significant. The voided spot on paper assay results may have
404 been influenced by surgical intervention and accompanying post-operative pain. Tail
405 vein injection of H-IPSE^{H03} did not affect voiding patterns in ifosfamide-treated mice at
406 all (data not shown). We did not allow mice to drink water during the 4-hour duration of
407 assay to avoid possible interference of dripping water with collection of urine on filter
408 paper. Post-operative pain in bladder wall-injected mice, as well as the lack of water
409 access, may have influenced voiding behavior independent of the effects of IPSE.

410 We previously demonstrated that H-IPSE^{H06} induces transcription of uroplakins in
411 the ifosfamide-injured bladder to a degree similar to or greater than MESNA (19).
412 Uroplakins are transmembrane proteins implicated in barrier functions, urothelial
413 proliferation and bladder regeneration (14). Co-incubation of a variety of urothelial cell
414 lines with H-IPSE^{H06} significantly increases cell proliferation (data not shown).
415 Moreover, co-incubation of the urothelial cell line MB49 with H-IPSE^{H03} induced a much
416 stronger proliferative response than H-IPSE^{H06}. The pro-proliferative effect of H-IPSE^{H03}

417 was nuclear localization sequence-dependent. This supports the notion that H-IPSE^{H03}
418 may upregulate urothelial repair mechanisms through translocation to the nucleus and
419 modulation of gene expression. Future work will be directed towards further quantifying
420 changes in uroplakin and related gene expression induced by H-IPSE^{H03}.

421 This study has several limitations. For instance, the mechanism by which H-
422 IPSE^{H03} targets and sequesters chemokines is poorly understood. It is possible that
423 IPSE's chemokine-binding properties may play a role in its therapeutic effects in the
424 ifosfamide-injured bladder independent of IL-4 effects. Furthermore, we have not
425 elucidated the mechanism by which IPSE exerts its effects outside the bladder. We
426 chiefly included experiments in which IPSE was delivered directly to the tissue of
427 interest. It is unclear how the mechanism of action of H-IPSE^{H03} is different when
428 administered in a local versus systemic fashion. For example, basophil and mast cell
429 recruitment to the bladder to release anti-inflammatory IL-4 may be modulated
430 differently based on the concentration of regional and systemic IPSE. Nuclear
431 translocation is an important component of the therapeutic effect of IPSE and we have
432 not yet investigated transcriptional regulation by H-IPSE^{H03}. It is also unclear whether
433 IPSE operates on a transcriptional level or whether there is a post-translational
434 component to its mechanism of action. Taken together, chemokine-binding and nuclear
435 translocation properties of IPSE are not well understood and may mediate some of the
436 effects reported in this manuscript. Further, we were unable to demonstrate histological
437 evidence to support our conclusions. As bladder wall injection was a surgical
438 intervention performed 24 hours prior to harvesting the tissues, there was significant
439 intramural artifact present in the sections that was more prominent than urothelial

440 changes. Post-surgical inflammation was more robust than the differences we
441 attempted to observe at this time point, which precluded accurate scoring.

442 Moreover, these experiments have not provided information as far as duration of
443 action of IPSE^{H03} in comparison to MESNA. However, MESNA has a well-known
444 protective effect against chemotherapy-induced cystitis with an equally well-established
445 duration of action. We have previously demonstrated that a single systemic dose of
446 ISPE^{H06} had a superior protective effect compared to 3 doses of MESNA (19). Duration
447 of action of H-IPSE^{H03} via systemic or local injection are areas of ongoing investigation.

448 In summary, we report the potential therapeutic application of a parasite-derived
449 protein, H-IPSE^{H03}, to treat hemorrhagic cystitis via bladder wall injection. Detrusor
450 injection of H-IPSE^{H03} can be readily applied to humans as other drugs such as
451 Botulinum Toxin A and bulking agents are delivered directly by bladder wall injection
452 (21, 25). Because we have found that IPSE modulates the host immune system to
453 dampen inflammation as well as pain responses, we speculate that this protein could
454 potentially be used for broader indications, such as interstitial cystitis and other bladder
455 pain syndromes.

456 **Acknowledgements**

457 We thank H. Gil Rushton and Hans G. Pohl for their support of urologic basic science
458 research at Children's National Medical Center.

459 **Grants**

460 This work was supported by funding from the Margaret A. Stirewalt Endowment and the
461 U.S. National Institutes of Health, National Institutes of Diabetes and Digestive and
462 Kidney Diseases (1R01DK113504).

463

- 466 1. **Ackert-Bicknell CL, Anderson LC, Sheehan S, Hill WG, Chang B, Churchill**
467 **GA, Chesler EJ, Korstanje R, Peters LL.** Aging Research Using Mouse Models.
468 In: *Current Protocols in Mouse Biology*. John Wiley & Sons, Inc., p. 95–133.
- 469 2. **Andriole GL, Sandlund JT, Miser JS, Arasi V, Linehan M, Magrath IT.** The
470 efficacy of mesna (2-mercaptoethane sodium sulfonate) as a uroprotectant in
471 patients with hemorrhagic cystitis receiving further oxazaphosphorine
472 chemotherapy. *J Clin Oncol* 5: 799–803, 1987.
- 473 3. **Bicer F, Altuntas CZ, Izgi K, Ozer A, Kavran M, Tuohy VK, Daneshgari F.**
474 Chronic pelvic allodynia is mediated by CCL2 through mast cells in an
475 experimental autoimmune cystitis model. *AJP Ren Physiol* 308: F103–F113,
476 2015.
- 477 4. **Bon K, Lichtensteiger CA, Wilson SG, Mogil JS.** Characterization of
478 cyclophosphamide cystitis, a model of visceral and referred pain, in the mouse:
479 Species and strain differences. *J Urol* 170: 1008–1012, 2003.
- 480 5. **Boucher M, Meen M, Codron JP, Coudore F, Kemeny JL, Eschaliere a.**
481 Cyclophosphamide-induced cystitis in freely-moving conscious rats: behavioral
482 approach to a new model of visceral pain. *J Urol* 164: 203–8, 2000.
- 483 6. **Chaplan SR, Bach FW, Pogrel JW, Chung JM, Yaksh TL.** Quantitative
484 assessment of tactile allodynia in the rat paw. *J Neurosci Methods* 53: 55–63,
485 1994.
- 486 7. **Delafosse L, Xu P, Durocher Y.** Comparative study of polyethylenimines for
487 transient gene expression in mammalian HEK293 and CHO cells. *J. Biotechnol.*
488 (2016). doi: 10.1016/j.jbiotec.2016.04.028.
- 489 8. **Falcone FH, Alcocer MJC, Okamoto-Uchida Y, Nakamura R.** Use of
490 humanized rat basophilic leukemia reporter cell lines as a diagnostic tool for
491 detection of allergen-specific IgE in allergic patients: time for a reappraisal? *Curr*
492 *Allergy Asthma Rep* 15: 67, 2015.
- 493 9. **Fu C-L, Odegaard JI, Herbert DR, Hsieh MH.** A Novel Mouse Model of
494 *Schistosoma haematobium* Egg-Induced Immunopathology. *PLoS Pathog* 8:
495 e1002605, 2012.
- 496 10. **Hader JE, Marzella L, Myers RA, Jacobs SC, Naslund MJ.** Hyperbaric oxygen
497 treatment for experimental cyclophosphamide-induced hemorrhagic cystitis. *J*
498 *Urol* 149: 1617–21, 1993.
- 499 11. **Hewitson JP, Grainger JR, Maizels RM.** Helminth immunoregulation: The role of
500 parasite secreted proteins in modulating host immunity. *Mol Biochem Parasitol*
501 167: 1–11, 2009.
- 502 12. **Hsieh Y-J, Fu C-L, Hsieh MH.** Helminth-Induced Interleukin-4 Abrogates

- 503 Invariant Natural Killer T Cell Activation-Associated Clearance of Bacterial
504 Infection. *Infect Immun* 82: 2087–2097, 2014.
- 505 13. **Knuhr K, Langhans K, Nyenhuis S, Viertmann K, Kildemoes AMO, Doenhoff**
506 **MJ, Haas H, Schramm G.** Schistosoma mansoni Egg-Released IPSE/alpha-1
507 Dampens Inflammatory Cytokine Responses via Basophil Interleukin (IL)-4 and
508 IL-13. *Front Immunol* 9: 2293, 2018.
- 509 14. **Lee G.** Uroplakins in the lower urinary tract. *Int Neurol J* 15: 4–12, 2011.
- 510 15. **Leventhal L, Strassle B.** A model of cystitis pain in the mouse. *Curr Protoc*
511 *Pharmacol* : 1–11, 2008.
- 512 16. **Lima MVA, Ferreira FV, Macedo FYB, de Castro Brito GA, Ribeiro RA.**
513 Histological changes in bladders of patients submitted to ifosfamide
514 chemotherapy even with mesna prophylaxis. *Cancer Chemother Pharmacol* 59:
515 643–650, 2007.
- 516 17. **Macedo FYB, Mourão LTC, Freitas HC, Lima RCP, Wong DVT, Oriá RB, Vale**
517 **ML, Brito GAC, Cunha FQ, Ribeiro RA.** Interleukin-4 modulates the
518 inflammatory response in ifosfamide-induced hemorrhagic cystitis. *Inflammation*
519 35: 297–307, 2012.
- 520 18. **Matz EL, Hsieh MH.** Review of Advances in Uroprotective Agents for
521 Cyclophosphamide- and Ifosfamide-induced Hemorrhagic Cystitis. *Urology* 100:
522 16–19, 2017.
- 523 19. **Mbanefo EC, Le L, Pennington LF, Odegaard JI, Jardetzky TS, Alouffi A,**
524 **Falcone FH, Hsieh MH.** Therapeutic exploitation of IPSE, a urogenital parasite-
525 derived host modulatory protein, for chemotherapy-induced hemorrhagic cystitis.
526 *FASEB J* 32: 000–000, 2018.
- 527 20. **Oguchi T, Funahashi Y, Yokoyama H, Nishizawa O, Goins WF, Goss JR,**
528 **Glorioso JC, Yoshimura N.** Effect of herpes simplex virus vector-mediated
529 interleukin-4 gene therapy on bladder overactivity and nociception. *Gene Ther* 20:
530 194–200, 2013.
- 531 21. **Oswald J, Riccabona M, Lusuardi L, Bartsch G, Radmayr C.** Prospective
532 comparison and 1-year follow-up of a single endoscopic subureteral
533 polydimethylsiloxane versus dextranomer/hyaluronic acid copolymer injection for
534 treatment of vesicoureteral reflux in children. *Urology* 60: 894–897, 2002.
- 535 22. **Pennington LF, Alouffi A, Mbanefo EC, Ray D, Heery DM, Jardetzky TS,**
536 **Hsieh MH, Falcone FH.** H-IPSE is a pathogen-secreted host nucleus infiltrating
537 protein (infiltrin) expressed exclusively by the Schistosoma haematobium egg
538 stage. *Infect Immun* 85: e00301-17, 2017.
- 539 23. **Ribeiro R, Lima Junior R, Leite C, Mota J, Macedo F, Lima M, Brito G.**
540 Chemotherapy-induced hemorrhagic cystitis: pathogenesis, pharmacological
541 approaches and new insights. *J Exp Integr Med* 2: 1, 2012.
- 542 24. **SAKURAI M, SAIJO N, SHINKAI T, EGUCHI K, SASAKI Y, TAMURA T, SANO**

- 543 **T, SUEMASU K, JETT JR.** The Protective Effect of 2-Mercapto-Ethane Sulfonate
544 (MESNA) on Hemorrhagic Cystitis Induced by High-Dose Ifosfamide Treatment
545 Tested by a Randomized Crossover Trial. *Jpn J Clin Oncol* 16: 153–156, 1986.
- 546 25. **Schulte-Baukloh H, Michael T, Stürzebecher B, Knispel HH.** Botulinum-A
547 Toxin Detrusor Injection as a Novel Approach in the Treatment of Bladder
548 Spasticity in Children with Neurogenic Bladder. *Eur Urol* 44: 139–143, 2003.
- 549 26. **Shepherd JD, Pringle LE, Barnett MJ, Klingemann HG, Reece DE, Phillips**
550 **GL.** Mesna versus hyperhydration for the prevention of cyclophosphamide-
551 induced hemorrhagic cystitis in bone marrow transplantation. *J Clin Oncol* 9:
552 2016–20, 1991.
- 553 27. **Smith P, Fallon RE, Mangan NE, Walsh CM, Saraiva M, Sayers JR, McKenzie**
554 **ANJ, Alcamì A, Fallon PG.** *Schistosoma mansoni* secretes a chemokine binding
555 protein with antiinflammatory activity. *J Exp Med* 202: 1319–25, 2005.
- 556 28. **Wan D, Ludolf F, Alanine DGW, Stretton O, Ali Ali E, Al-Barwary N, Wang X,**
557 **Doenhoff MJ, Mari A, Fitzsimmons CM, Dunne DW, Nakamura R, Oliveira**
558 **GC, Alcocer MJC, Falcone FH.** Use of Humanised Rat Basophilic Leukaemia
559 Cell Line RS-ATL8 for the Assessment of Allergenicity of *Schistosoma mansoni*
560 Proteins. *PLoS Negl. Trop. Dis.* (2014). doi: 10.1371/journal.pntd.0003124.
- 561 29. **Watanabe K, Muhoho ND, Mutua WR, Kiliku FM, Awazawa T, Moji K, Aoki Y.**
562 Assessment of Voiding Function in Inhabitants Infected with *Schistosoma*
563 *haematobium*. *J Trop Pediatr* 57: 263–268, 2011.
- 564 30. **Yu W, Ackert-Bicknell C, Larigakis JD, MacIver B, Steers WD, Churchill GA,**
565 **Hill WG, Zeidel ML.** Spontaneous voiding by mice reveals strain-specific lower
566 urinary tract function to be a quantitative genetic trait. *AJP Ren Physiol* 306:
567 F1296–F1307, 2014.
- 568

569 **Figure Legends**

570

571 **Figure 1:** Bladder wall injection technique. Mice were anesthetized with inhaled
572 isoflurane. Next their abdomens were depilated and cleaned, injected with local
573 anesthetic, and a midline laparotomy was performed. The bladder was exteriorized,
574 stabilized with a cotton applicator, and its wall injected with a 30 gauge needle.

575 **Figure 2:** (A) Western blots of purified H-IPSE^{H03} and H-IPSE^{H06} proteins demonstrate a
576 prominent band with a molecular weight of approximately 38-40 kDa. (B) RS-ATL8
577 basophil NF-AT activation in response to M-IPSE, H-IPSE^{H03} and H-IPSE^{H06}. Incubation
578 of IPSE with IgE-bearing basophils demonstrates that H-IPSE orthologs induce NF-AT
579 reporter gene expression comparable to M-IPSE.

580 **Figure 3:** Effect of H-IPSE^{H03} on bladder wet weights. Mice received a bladder wall
581 injection (A) or a tail vein injection (B) with or without H-IPSE^{H03} or a nuclear localization
582 sequence mutant of H-IPSE^{H03} (IPSE_{NLS}). Twenty-four hours later, mice were injected
583 with PBS (control) or ifosfamide (“ifosfamide” or “ifos”). Some mice received neutralizing
584 anti-IL4 antibody (α IL4) 30 minutes prior to ifosfamide. Bladders were collected and
585 weighed 12 hours following ifosfamide injection to assess for edema and hemorrhage.
586 **A.** Bladder wall injection of H-IPSE^{H03} significantly decreases ifosfamide-induced
587 increase in bladder wet weight in an IL-4- but not nuclear translocation-dependent
588 fashion. *p=0.02, **p<0.006, ***p<0.001. **B.** Tail vein injection of H-IPSE^{H03} non-
589 significantly decreases the ifosfamide-induced increase in BWW in an IL-4 but not NLS-
590 dependent fashion. Plotted data are pooled from 3 experiments. Error bars represent
591 means and one standard deviation. *p=0.01, **p=0.03, ***p<0.001.

592 **Figure 4:** The effect of IPSE bladder wall injections on evoked pain responses (referred
593 hyperalgesia). H-IPSE^{H03} bladder wall injection alleviates allodynia (referred
594 hyperalgesia) associated with hemorrhagic cystitis-associated pain in an IL-4 and NLS-
595 dependent manner. Plotted data are pooled from 3 experiments. Error bars represent
596 means and one standard deviation. *p=0.04, **p=0.02, ***p=0.01.

597 **Figure 5:** Voiding dysfunction caused by ifosfamide was alleviated by bladder wall
598 injections of H-IPSE^{H03}. Ifosfamide significantly decreased corner voiding (A & C). H-
599 IPSE^{H03} non-significantly restored the percentage of corner voids in ifosfamide-treated
600 mice (D). Administration of neutralizing α -IL4 antibody may reverse the non-significant
601 protective effect of H-IPSE^{H03} (E). Administration of H-IPSE^{H03} that cannot localize to the
602 nucleus has a similar effect on chemotherapy-exposed voiding patterns as wild type H-
603 IPSE^{H03}. Plotted data are pooled from 3 experiments. Error bars represent means and
604 one standard deviation. **p<0.01.

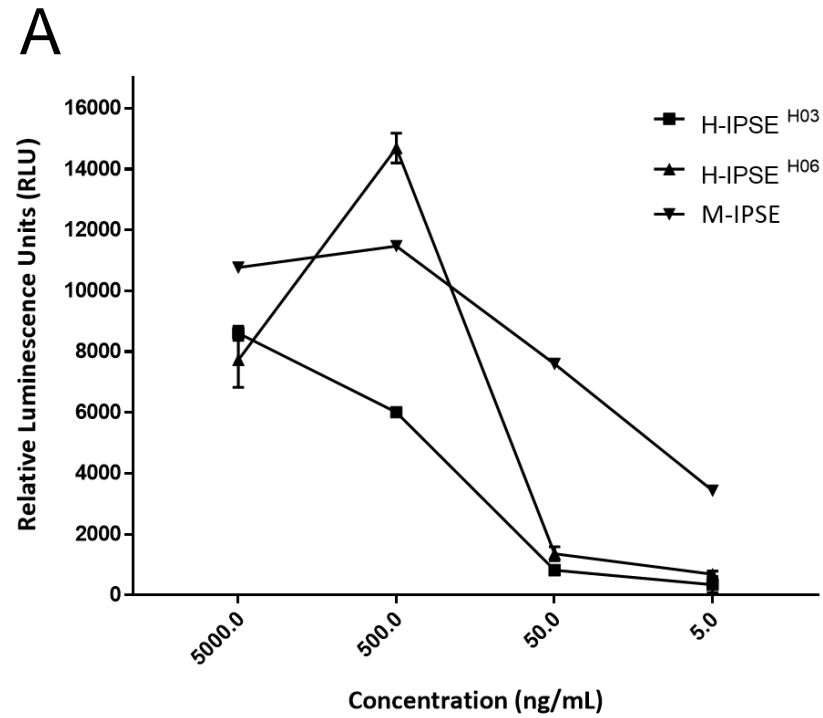
605 **Figure 6:** H-IPSE^{H03} co-incubation with MB49 cells induced proliferation in an NLS-
606 dependent fashion. (A) When co-incubated with H-IPSE^{H03}, the number of MB49 cells
607 was markedly increased versus control over 3 generations of cells. Significant increases
608 in proliferation were observed for both low (0.065 pmol) and high concentrations of H-
609 IPSE^{H03} (up to 65.5 pmol). (B) MB49 cellular proliferation was not increased compared
610 to controls by co-incubation with H-IPSE^{H03NLS}. Error bars represent means and one
611 standard deviation. *p<0.05, ***p<0.001.

AJP revision figures

Figure 1



Figure 2



B

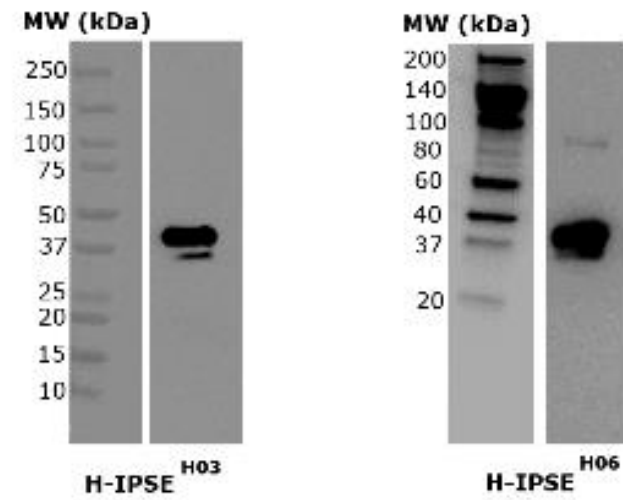


Figure 3

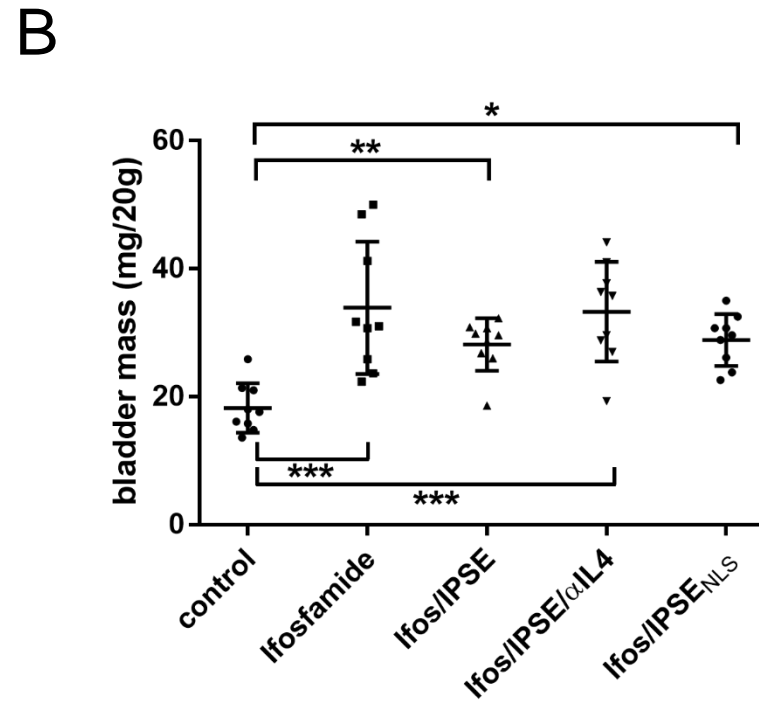
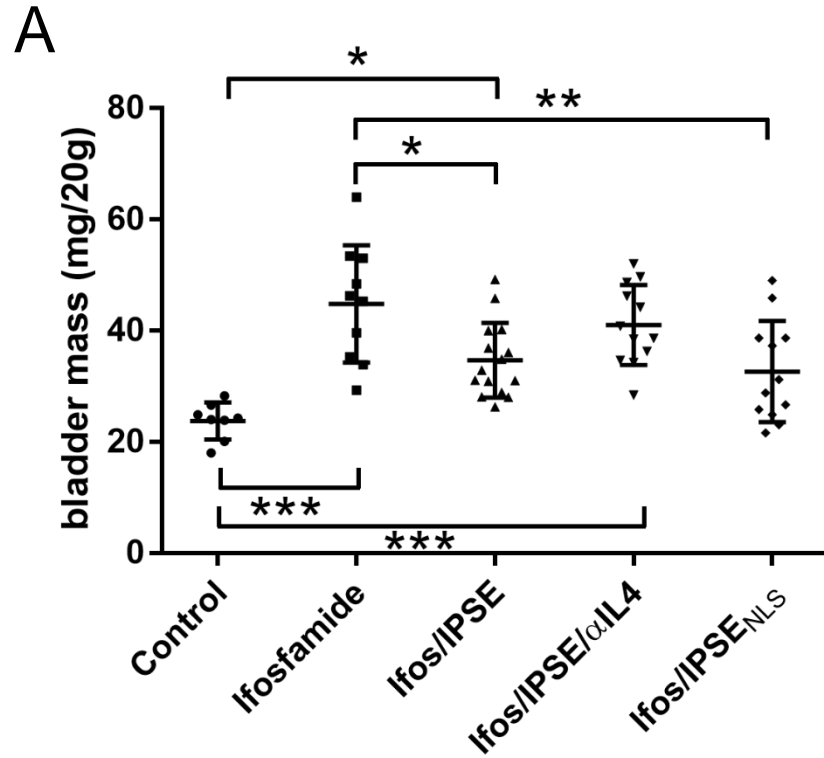


Figure 4

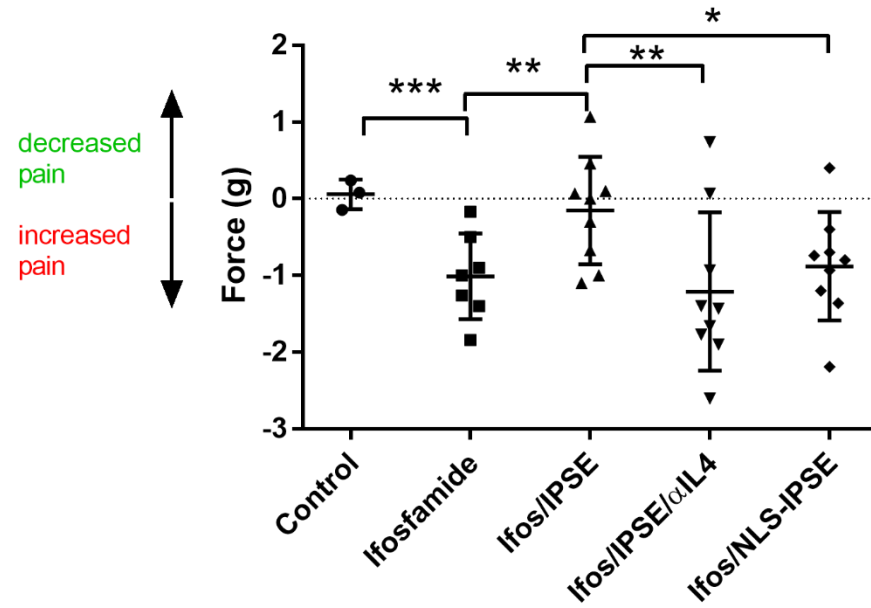


Figure 5

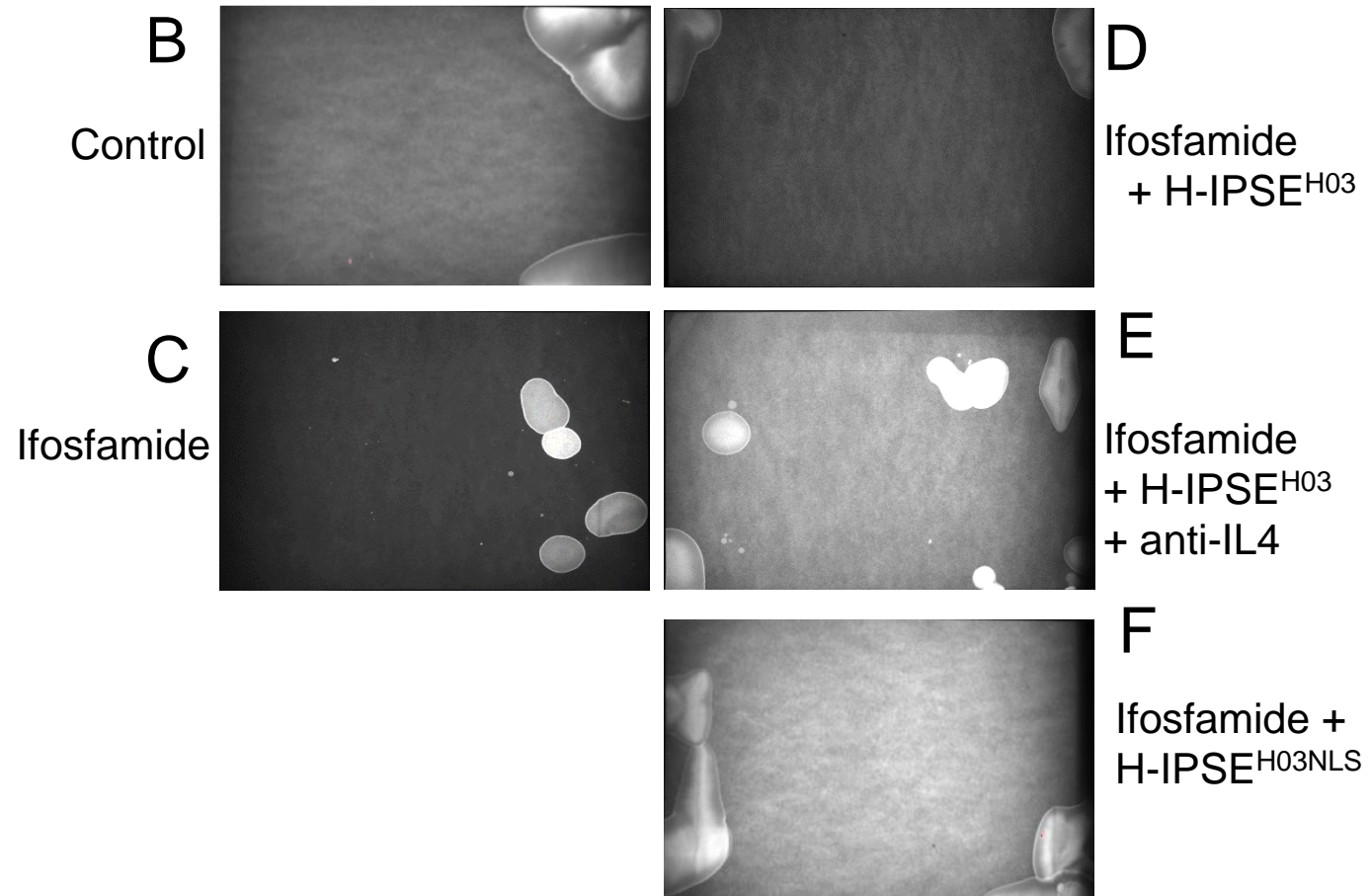
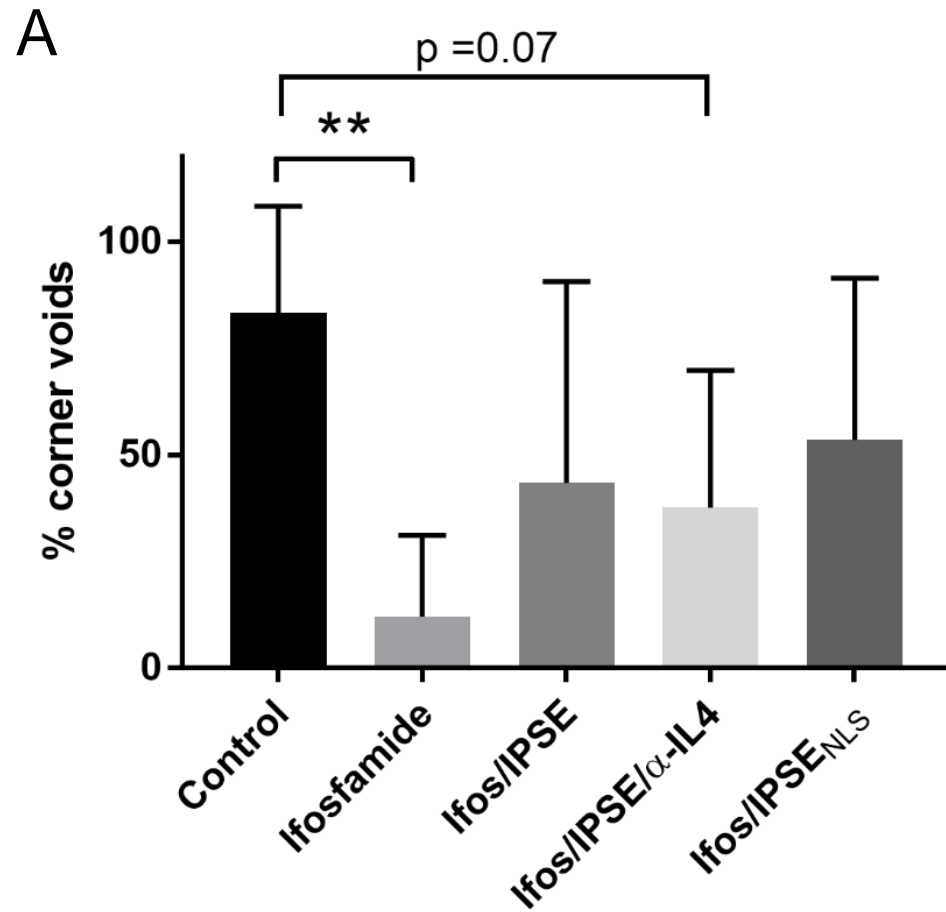


Figure 6

